

University of Nebraska - Lincoln

DigitalCommons@University of Nebraska - Lincoln

Kenneth Bloom Publications

Research Papers in Physics and Astronomy

9-4-2000

Search for New Particles Decaying to $t\bar{t}$ in $p\bar{p}$ Collisions at $\sqrt{s} = 1.8$ TeV

T. Affolder

Ernest Orlando Lawrence Berkeley National Laboratory, Berkeley, California

Kenneth A. Bloom

University of Nebraska-Lincoln, kenbloom@unl.edu

Collider Detector at Fermilab Collaboration

Follow this and additional works at: <https://digitalcommons.unl.edu/physicsbloom>



Part of the [Physics Commons](#)

Affolder, T.; Bloom, Kenneth A.; and Fermilab Collaboration, Collider Detector at, "Search for New Particles Decaying to $t\bar{t}$ in $p\bar{p}$ Collisions at $\sqrt{s} = 1.8$ TeV" (2000). *Kenneth Bloom Publications*. 103.
<https://digitalcommons.unl.edu/physicsbloom/103>

This Article is brought to you for free and open access by the Research Papers in Physics and Astronomy at DigitalCommons@University of Nebraska - Lincoln. It has been accepted for inclusion in Kenneth Bloom Publications by an authorized administrator of DigitalCommons@University of Nebraska - Lincoln.

Search for New Particles Decaying to $t\bar{t}$ in $p\bar{p}$ Collisions at $\sqrt{s} = 1.8$ TeV

T. Affolder,²¹ H. Akimoto,⁴³ A. Akopian,³⁶ M. G. Albrow,¹⁰ P. Amaral,⁷ S. R. Amendolia,³² D. Amidei,²⁴ K. Anikeev,²² J. Antos,¹ G. Apollinari,³⁶ T. Arisawa,⁴³ T. Asakawa,⁴¹ W. Ashmanskas,⁷ M. Atac,¹⁰ F. Azfar,²⁹ P. Azzi-Bacchetta,³⁰ N. Bacchetta,³⁰ M. W. Bailey,²⁶ S. Bailey,¹⁴ P. de Barbaro,³⁵ A. Barbaro-Galtieri,²¹ V. E. Barnes,³⁴ B. A. Barnett,¹⁷ M. Barone,¹² G. Bauer,²² F. Bedeschi,³² S. Belforte,⁴⁰ G. Bellettini,³² J. Bellinger,⁴⁴ D. Benjamin,⁹ J. Bensinger,⁴ A. Beretvas,¹⁰ J. P. Berge,¹⁰ J. Berryhill,⁷ B. Bevensee,³¹ A. Bhatti,³⁶ M. Binkley,¹⁰ D. Bisello,³⁰ R. E. Blair,² C. Blocker,⁴ K. Bloom,²⁴ B. Blumenfeld,¹⁷ S. R. Blusk,³⁵ A. Bocci,³² A. Bodek,³⁵ W. Bokhari,³¹ G. Bolla,³⁴ Y. Bonushkin,⁵ D. Bortoletto,³⁴ J. Boudreau,³³ A. Brandl,²⁶ S. van den Brink,¹⁷ C. Bromberg,²⁵ M. Brozovic,⁹ N. Bruner,²⁶ E. Buckley-Geer,¹⁰ J. Budagov,⁸ H. S. Budd,³⁵ K. Burkett,¹⁴ G. Busetto,³⁰ A. Byon-Wagner,¹⁰ K. L. Byrum,² M. Campbell,²⁴ W. Carithers,²¹ J. Carlson,²⁴ D. Carlsmith,⁴⁴ J. Cassada,³⁵ A. Castro,³⁰ D. Cauz,⁴⁰ A. Cerri,³² A. W. Chan,¹ P. S. Chang,¹ P. T. Chang,¹ J. Chapman,²⁴ C. Chen,³¹ Y. C. Chen,¹ M.-T. Cheng,¹ M. Chertok,³⁸ G. Chiarelli,³² I. Chirikov-Zorin,⁸ G. Chlachidze,⁸ F. Chlebana,¹⁰ L. Christofek,¹⁶ M. L. Chu,¹ S. Cihangir,¹⁰ C. I. Ciobanu,²⁷ A. G. Clark,¹³ A. Connolly,²¹ J. Conway,³⁷ J. Cooper,¹⁰ M. Cordelli,¹² J. Cranshaw,³⁹ D. Cronin-Hennessy,⁹ R. Cropp,²³ R. Culbertson,⁷ D. Dagenhart,⁴² F. DeJongh,¹⁰ S. Dell'Agnello,¹² M. Dell'Orso,³² R. Demina,¹⁰ L. Demortier,³⁶ M. Dennino,³ P. F. Derwent,¹⁰ T. Devlin,³⁷ J. R. Dittmann,¹⁰ S. Donati,³² J. Done,³⁸ T. Dorigo,¹⁴ N. Eddy,¹⁶ K. Einsweiler,²¹ J. E. Elias,¹⁰ E. Engels, Jr.,³³ W. Erdmann,¹⁰ D. Errede,¹⁶ S. Errede,¹⁶ Q. Fan,³⁵ R. G. Feild,⁴⁵ C. Ferretti,³² R. D. Field,¹¹ I. Fiori,³ B. Flaughner,¹⁰ G. W. Foster,¹⁰ M. Franklin,¹⁴ J. Freeman,¹⁰ J. Friedman,²² Y. Fukui,²⁰ S. Galeotti,³² M. Gallinaro,³⁶ T. Gao,³¹ M. Garcia-Sciveres,²¹ A. F. Garfinkel,³⁴ P. Gatti,³⁰ C. Gay,⁴⁵ S. Geer,¹⁰ D. W. Gerdes,²⁴ P. Giannetti,³² P. Giromini,¹² V. Glagolev,⁸ M. Gold,²⁶ J. Goldstein,¹⁰ A. Gordon,¹⁴ A. T. Goshaw,⁹ Y. Gotra,³³ K. Goulianos,³⁶ C. Green,³⁴ L. Groer,³⁷ C. Grosso-Pilcher,⁷ M. Guenther,³⁴ G. Guillian,²⁴ J. Guimaraes da Costa,²⁴ R. S. Guo,¹ C. Haber,²¹ E. Hafen,²² S. R. Hahn,¹⁰ C. Hall,¹⁴ T. Handa,¹⁵ R. Handler,⁴⁴ W. Hao,³⁹ F. Happacher,¹² K. Hara,⁴¹ A. D. Hardman,³⁴ R. M. Harris,¹⁰ F. Hartmann,¹⁸ K. Hatakeyama,³⁶ J. Hauser,⁵ J. Heinrich,³¹ A. Heiss,¹⁸ M. Herndon,¹⁷ B. Hinrichsen,²³ K. D. Hoffman,³⁴ C. Holck,³¹ R. Hollebeek,³¹ L. Holloway,¹⁶ R. Hughes,²⁷ J. Huston,²⁵ J. Huth,¹⁴ H. Ikeda,⁴¹ J. Incandela,¹⁰ G. Introzzi,³² J. Iwai,⁴³ Y. Iwata,¹⁵ E. James,²⁴ H. Jensen,¹⁰ M. Jones,³¹ U. Joshi,¹⁰ H. Kambara,¹³ T. Kamon,³⁸ T. Kaneko,⁴¹ K. Karr,⁴² H. Kasha,⁴⁵ Y. Kato,²⁸ T. A. Keaffaber,³⁴ K. Kelley,²² M. Kelly,²⁴ R. D. Kennedy,¹⁰ R. Kephart,¹⁰ D. Khazins,⁹ T. Kikuchi,⁴¹ M. Kirk,⁴ B. J. Kim,¹⁹ D. H. Kim,¹⁹ H. S. Kim,¹⁶ M. J. Kim,¹⁹ S. H. Kim,⁴¹ Y. K. Kim,²¹ L. Kirsch,⁴ S. Klimenko,¹¹ P. Koehn,²⁷ A. Köngeter,¹⁸ K. Kondo,⁴³ J. Konigsberg,¹¹ K. Kordas,²³ A. Korn,²² A. Korytov,¹¹ E. Kovacs,² J. Kroll,³¹ M. Kruse,³⁵ S. E. Kuhlmann,² K. Kurino,¹⁵ T. Kuwabara,⁴¹ A. T. Laasanen,³⁴ N. Lai,⁷ S. Lami,³⁶ S. Lammel,¹⁰ J. I. Lamoureux,⁴ M. Lancaster,²¹ G. Latino,³² T. LeCompte,² A. M. Lee IV,⁹ K. Lee,³⁹ S. Leone,³² J. D. Lewis,¹⁰ M. Lindgren,⁵ T. M. Liss,¹⁶ J. B. Liu,³⁵ Y. C. Liu,¹ N. Lockyer,³¹ J. Loken,²⁹ M. Loretto,³⁰ D. Lucchesi,³⁰ P. Lukens,¹⁰ S. Lusin,⁴⁴ L. Lyons,²⁹ J. Lys,²¹ R. Madrak,¹⁴ K. Maeshima,¹⁰ P. Maksimovic,¹⁴ L. Malferrari,³ M. Mangano,³² M. Mariotti,³⁰ G. Martignon,³⁰ A. Martin,⁴⁵ J. A. J. Matthews,²⁶ J. Mayer,²³ P. Mazzanti,³ K. S. McFarland,³⁵ P. McIntyre,³⁸ E. McKigney,³¹ M. Menguzzato,³⁰ A. Menzione,³² C. Mesropian,³⁶ T. Miao,¹⁰ R. Miller,²⁵ J. S. Miller,²⁴ H. Minato,⁴¹ S. Miscetti,¹² M. Mishina,²⁰ G. Mitselmakher,¹¹ N. Moggi,³ E. Moore,²⁶ R. Moore,²⁴ Y. Morita,²⁰ A. Mukherjee,¹⁰ T. Muller,¹⁸ A. Munar,³² P. Murat,¹⁰ S. Murgia,²⁵ M. Musy,⁴⁰ J. Nachtman,⁵ S. Nahn,⁴⁵ H. Nakada,⁴¹ T. Nakaya,⁷ I. Nakano,¹⁵ C. Nelson,¹⁰ D. Neuberger,¹⁸ C. Newman-Holmes,¹⁰ C.-Y. P. Ngan,²² P. Nicolaidi,⁴⁰ H. Niu,⁴ L. Nodulman,² A. Nomerotski,¹¹ S. H. Oh,⁹ T. Ohmoto,¹⁵ T. Ohsugi,¹⁵ R. Oishi,⁴¹ T. Okusawa,²⁸ J. Olsen,⁴⁴ C. Pagliarone,³² F. Palmonari,³² R. Paoletti,³² V. Papadimitriou,³⁹ S. P. Pappas,⁴⁵ D. Partos,⁴ J. Patrick,¹⁰ G. Pauletta,⁴⁰ M. Paulini,²¹ C. Paus,²² L. Pescara,³⁰ T. J. Phillips,⁹ G. Piacentino,³² K. T. Pitts,¹⁶ R. Plunkett,¹⁰ A. Pompos,³⁴ L. Pondrom,⁴⁴ G. Pope,³³ M. Popovic,²³ F. Prokoshin,⁸ J. Proudfoot,² F. Ptohos,¹² G. Punzi,³² K. Ragan,²³ A. Rakitine,²² D. Reher,²¹ A. Reichold,²⁹ W. Riegler,¹⁴ A. Ribon,³⁰ F. Rimondi,³ L. Ristori,³² W. J. Robertson,⁹ A. Robinson,²³ T. Rodrigo,⁶ S. Rolli,⁴² L. Rosenson,²² R. Roser,¹⁰ R. Rossin,³⁰ W. K. Sakumoto,³⁵ D. Saltzberg,⁵ A. Sansoni,¹² L. Santi,⁴⁰ H. Sato,⁴¹ P. Savard,²³ P. Schlabach,¹⁰ E. E. Schmidt,¹⁰ M. P. Schmidt,⁴⁵ M. Schmitt,¹⁴ L. Scodellaro,³⁰ A. Scott,⁵ A. Scribano,³² S. Segler,¹⁰ S. Seidel,²⁶ Y. Seiya,⁴¹ A. Semenov,⁸ F. Semeria,³ T. Shah,²² M. D. Shapiro,²¹ P. F. Shepard,³³ T. Shibayama,⁴¹ M. Shimojima,⁴¹ M. Shochet,⁷ J. Siegrist,²¹ G. Signorelli,³² A. Sill,³⁹ P. Sinervo,²³ P. Singh,¹⁶ A. J. Slaughter,⁴⁵ K. Sliwa,⁴² C. Smith,¹⁷ F. D. Snider,¹⁰ A. Solodsky,³⁶ J. Spalding,¹⁰ T. Speer,¹³ P. Sphicas,²² F. Spinella,³² M. Spiropulu,¹⁴ L. Spiegel,¹⁰ J. Steele,⁴⁴ A. Stefanini,³² J. Strologas,¹⁶ F. Strumia,¹³ D. Stuart,¹⁰ K. Sumorok,²² T. Suzuki,⁴¹ T. Takano,²⁸ R. Takashima,¹⁵ K. Takikawa,⁴¹ P. Tamburello,⁹

M. Tanaka,⁴¹ B. Tannenbaum,⁵ W. Taylor,²³ M. Tecchio,²⁴ P.K. Teng,¹ K. Terashi,⁴¹ S. Tether,²² D. Theriot,¹⁰ R. Thurman-Keup,² P. Tipton,³⁵ S. Tkaczyk,¹⁰ K. Tollefson,³⁵ A. Tollestrup,¹⁰ H. Toyoda,²⁸ W. Trischuk,²³ J.F. de Troconiz,¹⁴ J. Tseng,²² N. Turini,³² F. Ukegawa,⁴¹ T. Vaiciulis,³⁵ J. Valls,³⁷ S. Vejcek III,¹⁰ G. Velev,¹⁰ R. Vidal,¹⁰ R. Vilar,⁶ I. Volobouev,²¹ D. Vucinic,²² R.G. Wagner,² R.L. Wagner,¹⁰ J. Wahl,⁷ N.B. Wallace,³⁷ A.M. Walsh,³⁷ C. Wang,⁹ C.H. Wang,¹ M.J. Wang,¹ T. Watanabe,⁴¹ D. Waters,²⁹ T. Watts,³⁷ R. Webb,³⁸ H. Wenzel,¹⁸ W.C. Wester III,¹⁰ A.B. Wicklund,² E. Wicklund,¹⁰ H.H. Williams,³¹ P. Wilson,¹⁰ B.L. Winer,²⁷ D. Winn,²⁴ S. Wolbers,¹⁰ D. Wolinski,²⁴ J. Wolinski,²⁵ S. Wolinski,²⁴ S. Worm,²⁶ X. Wu,¹³ J. Wyss,³² A. Yagil,¹⁰ W. Yao,²¹ G.P. Yeh,¹⁰ P. Yeh,¹ J. Yoh,¹⁰ C. Yosef,²⁵ T. Yoshida,²⁸ I. Yu,¹⁹ S. Yu,³¹ A. Zanetti,⁴⁰ F. Zetti,²¹ and S. Zucchelli³

(CDF Collaboration)

¹*Institute of Physics, Academia Sinica, Taipei, Taiwan 11529, Republic of China*

²*Argonne National Laboratory, Argonne, Illinois 60439*

³*Istituto Nazionale di Fisica Nucleare, University of Bologna, I-40127 Bologna, Italy*

⁴*Brandeis University, Waltham, Massachusetts 02254*

⁵*University of California at Los Angeles, Los Angeles, California 90024*

⁶*Instituto de Fisica de Cantabria, University of Cantabria, 39005 Santander, Spain*

⁷*Enrico Fermi Institute, University of Chicago, Chicago, Illinois 60637*

⁸*Joint Institute for Nuclear Research, RU-141980 Dubna, Russia*

⁹*Duke University, Durham, North Carolina 27708*

¹⁰*Fermi National Accelerator Laboratory, Batavia, Illinois 60510*

¹¹*University of Florida, Gainesville, Florida 32611*

¹²*Laboratori Nazionali di Frascati, Istituto Nazionale di Fisica Nucleare, I-00044 Frascati, Italy*

¹³*University of Geneva, CH-1211 Geneva 4, Switzerland*

¹⁴*Harvard University, Cambridge, Massachusetts 02138*

¹⁵*Hiroshima University, Higashi-Hiroshima 724, Japan*

¹⁶*University of Illinois, Urbana, Illinois 61801*

¹⁷*The Johns Hopkins University, Baltimore, Maryland 21218*

¹⁸*Institut für Experimentelle Kernphysik, Universität Karlsruhe, 76128 Karlsruhe, Germany*

¹⁹*Korean Hadron Collider Laboratory, Kyungpook National University, Taegu, 702-701, Korea,*

Seoul National University, Seoul 151-742, Korea,

and SungKyunKwan University, Suwon 440-746, Korea

²⁰*High Energy Accelerator Research Organization (KEK), Tsukuba, Ibaraki 305, Japan*

²¹*Ernest Orlando Lawrence Berkeley National Laboratory, Berkeley, California 94720*

²²*Massachusetts Institute of Technology, Cambridge, Massachusetts 02139*

²³*Institute of Particle Physics, McGill University, Montreal H3A 2T8, Canada,*

and University of Toronto, Toronto M5S 1A7, Canada

²⁴*University of Michigan, Ann Arbor, Michigan 48109*

²⁵*Michigan State University, East Lansing, Michigan 48824*

²⁶*University of New Mexico, Albuquerque, New Mexico 87131*

²⁷*The Ohio State University, Columbus, Ohio 43210*

²⁸*Osaka City University, Osaka 588, Japan*

²⁹*University of Oxford, Oxford OX1 3RH, United Kingdom*

³⁰*Universita di Padova, Istituto Nazionale di Fisica Nucleare, Sezione di Padova, I-35131 Padova, Italy*

³¹*University of Pennsylvania, Philadelphia, Pennsylvania 19104*

³²*Istituto Nazionale di Fisica Nucleare, University and Scuola Normale Superiore di Pisa, I-56100 Pisa, Italy*

³³*University of Pittsburgh, Pittsburgh, Pennsylvania 15260*

³⁴*Purdue University, West Lafayette, Indiana 47907*

³⁵*University of Rochester, Rochester, New York 14627*

³⁶*Rockefeller University, New York, New York 10021*

³⁷*Rutgers University, Piscataway, New Jersey 08855*

³⁸*Texas A&M University, College Station, Texas 77843*

³⁹*Texas Tech University, Lubbock, Texas 79409*

⁴⁰*Istituto Nazionale de Fisica Nucleare, University of Trieste/Udine, Italy*

⁴¹*University of Tsukuba, Tsukuba, Ibaraki 305, Japan*

⁴²*Tufts University, Medford, Massachusetts 02155*

⁴³*Waseda University, Tokyo 169, Japan*

⁴⁴*University of Wisconsin, Madison, Wisconsin 53706*

⁴⁵*Yale University, New Haven, Connecticut 06520*

(Received 28 February 2000)

We use 106 pb^{-1} of data collected with the Collider Detector at Fermilab to search for narrow-width, vector particles decaying to a top and an antitop quark. Model independent upper limits on the cross section for narrow, vector resonances decaying to $t\bar{t}$ are presented. At the 95% confidence level, we exclude the existence of a leptophobic Z' boson in a model of top-color-assisted technicolor with mass $M_{Z'} < 480 \text{ GeV}/c^2$ for natural width $\Gamma = 0.012M_{Z'}$, and $M_{Z'} < 780 \text{ GeV}/c^2$ for $\Gamma = 0.04M_{Z'}$.

PACS numbers: 14.65.Ha, 13.85.Ni, 13.85.Qk

In this Letter, we present a model-independent search for narrow, vector resonances decaying to $t\bar{t}$. This search is sensitive to, for example, a Z' predicted by top-color-assisted technicolor [1,2]. This model anticipates that the explanation of spontaneous electroweak symmetry breaking is related to the observed fermion masses, and that the large value of the top quark mass suggests the introduction of new strong dynamics into the standard model. It accounts for the large top quark mass by predicting the existence of a residual global symmetry $\text{SU}(3) \times \text{U}(1)$ at energies below 1 TeV. The $\text{SU}(3)$ results in the generation of top gluons which we have searched for previously in the $b\bar{b}$ channel [3]. The $\text{U}(1)$ gives the Z' we search for here. In one model [2], the Z' decays exclusively to quarks (leptophobic) resulting in a large cross section for $t\bar{t}$. The only previous measurement of the $t\bar{t}$ invariant mass spectrum did not include a search for narrow resonances [4].

With the z axis defined along the proton beam, the Collider Detector at Fermilab (CDF) coordinate system defines ϕ as the azimuthal angle in the transverse plane, θ as the polar angle, and pseudorapidity η as $-\ln(\tan \frac{\theta}{2})$. The central tracking chamber (CTC), immersed in a 1.4-T solenoidal magnetic field, is used to measure the momenta of charged particles. The precision track reconstruction of the silicon microstrip vertex detector (SVX), located immediately outside the beam pipe and within the CTC, is used for the detection of displaced secondary vertices resulting from b -quark decays. Electromagnetic and hadronic calorimeters, located beyond the CTC and superconducting solenoid, measure energy out to $|\eta|$ of 4.2. Drift chambers used for muon detection reside outside the calorimetry. A more detailed description of the CDF detector can be found elsewhere [5,6].

Standard model $t\bar{t}$ production in $p\bar{p}$ collisions at a center of mass energy of $\sqrt{s} = 1.8 \text{ TeV}$ is approximately 90% $q\bar{q}$ annihilation with the remaining 10% attributable to gluon-gluon fusion. Each top quark is expected to decay almost exclusively to Wb . The present search focuses on the $t\bar{t}$ event topology in which one W boson decays hadronically while the other decays to an electron or muon and its corresponding neutrino. Accordingly, $t\bar{t}$ candidates in this “lepton + jets” channel are characterized by a single lepton, missing transverse energy, \cancel{E}_T [7], due to the undetected neutrino, and at least four jets from the fragmentation of the final state quarks. Furthermore, a jet resulting from a b -quark can be identified (or “tagged”) as such by the reconstruction of a secondary vertex from the b hadron decay using the SVX, or by using the soft lepton

tagging (SLT) algorithm to find an additional lepton from a semileptonic b decay [6,8].

Events included in our measurement of the $t\bar{t}$ invariant mass spectrum must first contain a central ($|\eta| < 1.0$), isolated, highly energetic electron or muon. Electrons are required to have $E_T > 20 \text{ GeV}$, and muons $P_T > 20 \text{ GeV}/c$ [7]. Events must also include at least 20 GeV of \cancel{E}_T , and at least four jets with $|\eta| < 2.0$ and measured $E_T > 15 \text{ GeV}$. To increase the acceptance for $t\bar{t}$ events, the requirements for the fourth jet are relaxed to measured $E_T > 8 \text{ GeV}$ and $|\eta| < 2.4$ in events where at least one of the leading three jets is tagged by the SVX or SLT algorithms. In 106 pb^{-1} of data, we observe 83 events which satisfy these requirements.

This method builds upon the techniques developed for the top quark mass measurement [9] by fitting each event to the hypothesis of $t\bar{t}$ production followed by decay in the lepton + jets channel:

$$\begin{aligned} p\bar{p} &\rightarrow t\bar{t}\xi, & t &\rightarrow W^+b \rightarrow \ell^+ \nu_\ell (\text{or } q\bar{q}')b, \\ & & \bar{t} &\rightarrow W^- \bar{b} \rightarrow q\bar{q}' (\text{or } \ell^- \bar{\nu}_\ell) \bar{b}. \end{aligned}$$

The four-momenta of these 13 objects fully describe a $t\bar{t}$ event. The three-momenta of the charged lepton and four jets are measured directly. To compute the energies of these objects, the b and \bar{b} quark masses are taken to be $5 \text{ GeV}/c^2$, the q and \bar{q}' masses are taken to be $0.5 \text{ GeV}/c^2$, and the charged lepton mass is assigned according to its identification as either an electron or a muon. The components of transverse momentum for the recoiling system, ξ , are measured directly from extra jets in the event and unclustered energy deposits that are not included in lepton or jet energies. The transverse momentum components of the neutrino are computed by requiring that the total E_T in the event sums to zero. While the neutrino is assumed to be massless, its longitudinal momentum is a free parameter in the kinematic fit in which the $q\bar{q}'$ and $\ell\nu$ invariant masses are constrained to equal the W boson mass. We perform a kinematic fit to the production and decay of the $t\bar{t}$ pair as described by the decay chain shown above. This fitting procedure, which depends on the minimization of a χ^2 expression [10], allows the lepton energy, the jet energies, and the unclustered energy to vary within their respective uncertainties. The fitted results for these values determine the t and \bar{t} four-momenta, from which the $t\bar{t}$ invariant mass ($M_{t\bar{t}}$) can be computed. To improve the $M_{t\bar{t}}$ resolution, we also constrain the two

Wb invariant masses to a top mass of $175 \text{ GeV}/c^2$ [11]. We use only the four highest E_T jets, leading to 12 combinations for assigning jets to the b , \bar{b} , and hadronic W daughters. However, because we measure only the transverse component of the total energy, a twofold ambiguity in the longitudinal component of the neutrino momentum results in 24 combinations. We further require SVX or SLT-tagged jets to be assigned to b quarks, thereby reducing the number of combinations.

Electron energies and muon momenta are measured with the calorimeter and tracking chambers, respectively [12]. Jet energies are corrected for absolute energy scale calibration, contributions from the underlying event and multiple interactions, as well as energy losses in cracks between detector components and outside the clustering cone [13]. Additional corrections are necessary for assumed b quarks from top decays [10].

Using Monte Carlo simulations of signal and background events, we explored several event selection criteria in an attempt to optimize our discovery potential [14]. Of the 24 possibilities for each event, we select the $M_{t\bar{t}}$ value which corresponds to the configuration with the lowest χ^2 . To reduce the probability of selecting configurations with incorrect parton assignments which tend to yield artificially low values of $M_{t\bar{t}}$, we refit each event after releasing the constraint that the Wb invariant mass be equal to $175 \text{ GeV}/c^2$ and demand that the fit for this particular configuration return a value for the top quark mass between $150 \text{ GeV}/c^2$ and $200 \text{ GeV}/c^2$. To further reduce incorrect combinations and to increase discovery potential for a new particle decaying to $t\bar{t}$, we apply a χ^2 cut. For narrow width $t\bar{t}$ resonances, simulation predicts that the width of the $M_{t\bar{t}}$ spectrum is $\sim 6\%$ of the resonance mass for cases in which the correct jet configuration is selected. For resonances with a natural width Γ that is significantly less than 6% of the nominal mass, the CDF detector resolution will dominate and the resonances will all have approximately the same shape (shown in the inset of Fig. 1 for a mass of $500 \text{ GeV}/c^2$). At low $M_{t\bar{t}}$, the presence of residual events with incorrect parton assignments is evident in this figure.

The selection criteria described above eliminate an additional 20 events from our data sample and the resulting $M_{t\bar{t}}$ spectrum is shown in Fig. 1, along with the expected standard model $t\bar{t}$ and QCD $W + \text{jets}$ background shapes normalized to the data. While the non- $t\bar{t}$ background is dominated by $W + \text{jets}$ events, it also includes contributions from multijet $b\bar{b}$ events with one jet misidentified as a lepton, $Z + \text{jets}$ events, events with a boson pair, and single-top production. However, it has been shown that the VECBOS [15] $W + \text{jets}$ shape alone is sufficient in modeling the entire non- $t\bar{t}$ background spectrum [9,16]. Standard model $t\bar{t}$ is modeled with the HERWIG Monte Carlo program [17] and a CDF detector simulation. For this analysis, the expected non- $t\bar{t}$ background prediction of 31.1 ± 8.5 events is calculated as in Ref. [10], but accounts for differences in selection criteria. We find that the

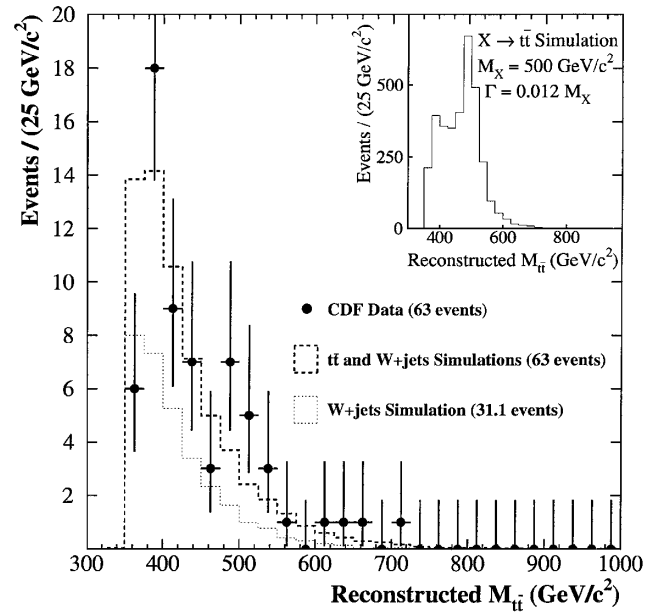


FIG. 1. The observed $M_{t\bar{t}}$ spectrum (points) compared to the QCD $W + \text{jets}$ background (fine dashes) and the total standard model prediction including both QCD $W + \text{jets}$ and $t\bar{t}$ production (thick dashes). The $t\bar{t}$ prediction has been normalized such that the number of events in the total standard model prediction is equal to the number of events in the data. The inset shows the expected $M_{t\bar{t}}$ shape resulting from the simulation of a narrow, vector $X \rightarrow t\bar{t}$ resonance ($M_X = 500 \text{ GeV}/c^2$, $\Gamma = 0.012 M_X$) in the CDF detector.

$M_{t\bar{t}}$ distribution of 63 data events yields a Kolmogorov-Smirnov probability of 16% when compared to the hypothesis that the spectrum is composed of standard model $t\bar{t}$ production and the predicted rate of non- $t\bar{t}$ background events, as shown in Fig. 1. Furthermore, the measured rate of $t\bar{t}$ production is consistent with previous measurements using the same data [18,19].

Because we cannot present evidence for a narrow $t\bar{t}$ resonance, we establish upper limits on the production cross section for a new vector particle, X , of mass M_X decaying to $t\bar{t}$. For natural widths $\Gamma = 0.012 M_X$ and $\Gamma = 0.04 M_X$, and for each M_X between $400 \text{ GeV}/c^2$ and $1 \text{ TeV}/c^2$ in increments of $50 \text{ GeV}/c^2$, we perform a binned-likelihood fit of the data. To determine the likelihood function for a given M_X and Γ , we fit the $M_{t\bar{t}}$ spectrum from the data to the expected Monte Carlo shapes for both the $t\bar{t}$ and QCD $W + \text{jets}$ background sources as well as a resonance signal $X \rightarrow t\bar{t}$ which we model using $Z' \rightarrow t\bar{t}$ in PYTHIA [20].

Our analysis is subject to several sources of systematic uncertainty on the expected shape of background and signal $M_{t\bar{t}}$ spectra and/or the signal acceptance rate. Treating these two types of systematic effects separately, we establish the magnitude of each source through a Monte Carlo procedure which quantifies the effect of varying the source of uncertainty by 1 standard deviation. We determine the uncertainty contributions due to the jet E_T scale, initial

TABLE I. The percent systematic uncertainty in $\sigma_X B\{X \rightarrow t\bar{t}\}$ from various sources.

| Source | $M_X(\text{GeV}/c^2)$ | | |
|---|-----------------------|------|-------|
| | 400 | 600 | 800 |
| Jet E_T alone | 6.1 | 6.2 | 4.4 |
| M_{top} alone | 22 | 3.1 | 8.7 |
| Jet E_T and M_{top} combined | 28 | 9.3 | 13 |
| Initial state radiation | 14 | 4.2 | 5.6 |
| Final state radiation | 19 | 16 | 12 |
| b -tagging bias | 4.6 | 0.79 | 0.85 |
| PDF | 11 | 5.5 | 4.8 |
| QCD background shape | 1.3 | 0.17 | 0.045 |
| Additional acceptance effects | 5.3 | 5.3 | 5.3 |
| Luminosity | 4.0 | 4.0 | 4.0 |
| Total | 39 | 21 | 20 |

and final state gluon radiation, and the non- $t\bar{t}$ background spectrum using methods described in Ref. [10]. The uncertainty in the measurements of the top quark mass [11] and total integrated luminosity [21] are included in our study of systematic effects, as well as the uncertainty due to the choice of parton distribution functions (PDF). The remaining sources of systematic uncertainty considered are all small and include trigger efficiency, lepton identification, tracking efficiency, z -vertex efficiency, and Monte Carlo statistics. The uncertainties resulting from jet E_T scale and top quark mass are correlated, and we conservatively take this correlation to be 100%.

The percent uncertainty in $\sigma_X B\{X \rightarrow t\bar{t}\}$ is listed in Table I for each of the systematic sources at several different resonance masses. The systematic effect due to uncertainty in the top quark mass (M_{top}) is dominant at low M_X , whereas the effect due to the uncertainty in modeling final state radiation dominates at large M_X . To ensure that our estimates are conservative, the systematic uncertainty is taken to be a constant number of pb below the value of $\sigma_X B\{X \rightarrow t\bar{t}\}$ corresponding to the 95% C.L. limit obtained with statistical uncertainties only [14]. That constant is the estimate of the systematic uncertainty at the 95% C.L. limit. Above the same value of $\sigma_X B\{X \rightarrow t\bar{t}\}$, we use a systematic uncertainty that rises with $\sigma_X B\{X \rightarrow t\bar{t}\}$ at the fixed percent rate listed in Table I.

For each resonance mass and width, we convolute the statistical likelihood shape with the Gaussian total systematic uncertainty and extract the 95% C.L. upper limit on $\sigma_X B\{X \rightarrow t\bar{t}\}$ which is listed in Table II and shown in Fig. 2. The systematic uncertainties increase the 95% C.L. upper limit by 27% for $M_X = 400 \text{ GeV}/c^2$, but only 7% (6%) for $M_X = 600$ (800) GeV/c^2 because statistical uncertainties dominate the likelihood. Also shown in Fig. 2 are the theoretical predictions for cross-section times branching ratio for a leptophobic Z' with natural width $\Gamma = 0.012M_{Z'}$ and $\Gamma = 0.04M_{Z'}$ [2]. At 95% confidence, we exclude the existence of a leptophobic top-

TABLE II. The 95% C.L. upper limit on the cross section times branching ratio for vector particles decaying to $t\bar{t}$, as a function of mass, for two natural widths.

| M_X (GeV/c^2) | 95% C.L. upper limit $\sigma_X B\{X \rightarrow t\bar{t}\}$ (pb) | |
|-------------------------------|---|------------------------|
| | for $\Gamma = 0.012M_X$ | for $\Gamma = 0.04M_X$ |
| 400 | 6.60 | 6.51 |
| 450 | 5.21 | 6.32 |
| 500 | 7.31 | 6.97 |
| 550 | 3.58 | 3.95 |
| 600 | 1.92 | 2.23 |
| 650 | 1.82 | 1.92 |
| 700 | 1.53 | 1.63 |
| 750 | 1.21 | 1.27 |
| 800 | 0.97 | 1.07 |
| 850 | 0.91 | 1.02 |
| 900 | 0.93 | 1.08 |
| 950 | 1.00 | 1.10 |
| 1000 | 1.00 | 1.23 |

color Z' with mass $M_{Z'} < 480 \text{ GeV}/c^2$ for natural width $\Gamma = 0.012M_{Z'}$, and mass $M_{Z'} < 780 \text{ GeV}/c^2$ for $\Gamma = 0.04M_{Z'}$. For larger widths, detector resolution will no longer be the dominant factor in determining the Z' signal shape, so our limits are no longer applicable.

In conclusion, after investigating 106 pb^{-1} of data collected at CDF, we find no evidence for a $t\bar{t}$ resonance and establish upper limits on cross-section times branching ratio for narrow resonances. We have used these limits to constrain a model of top-color-assisted technicolor.

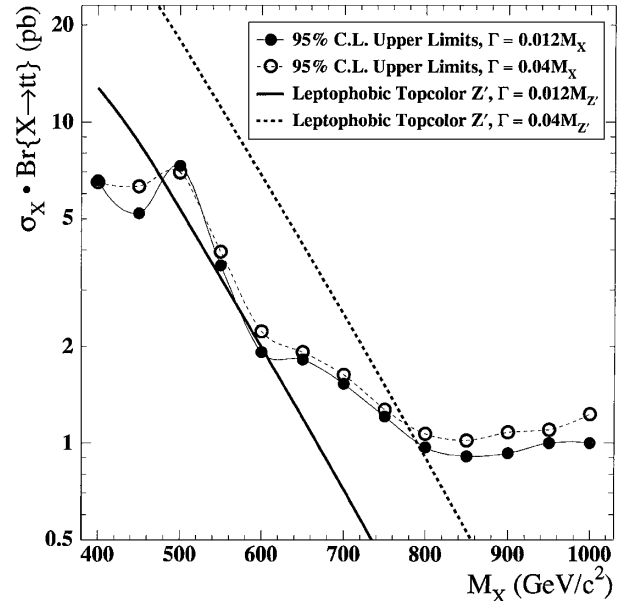


FIG. 2. The 95% C.L. upper limits on $\sigma_X B\{X \rightarrow t\bar{t}\}$ as a function of mass (solid and open points) compared to the cross section for a leptophobic top-color Z' (thick solid and dashed curves) for two resonance widths ($\Gamma = 0.012M_{Z'}$ and $\Gamma = 0.04M_{Z'}$).

We thank the Fermilab staff and the technical staffs of the participating institutions for their vital contributions. This work is supported by the U.S. Department of Energy and the National Science Foundation; the Natural Sciences and Engineering Research Council of Canada; the Istituto Nazionale di Fisica Nucleare of Italy; the Ministry of Education, Science and Culture of Japan; the National Science Council of the Republic of China; and the A. P. Sloan Foundation.

-
- [1] C. T. Hill, Phys. Lett. B **345**, 483 (1995); C. T. Hill and S. J. Parke, Phys. Rev. D **49**, 4454 (1994).
 - [2] R. M. Harris, C. T. Hill, and S. J. Parke, Fermilab Report No. Fermilab-FN-687; hep-ph/9911288, 1999.
 - [3] F. Abe *et al.*, Phys. Rev. Lett. **82**, 2038 (1999).
 - [4] B. Abbott *et al.*, Phys. Rev. D **58**, 052001 (1998).
 - [5] F. Abe *et al.*, Nucl. Instrum. Methods Phys. Res., Sect. A **271**, 387 (1988).
 - [6] F. Abe *et al.*, Phys. Rev. D **50**, 2966 (1994).
 - [7] The transverse momentum of a particle is $P_T = P \sin\theta$. The analogous quantity using calorimeter energies, defined as $E_T = E \sin\theta$, is called transverse energy. Missing transverse energy \cancel{E}_T is defined as $-\sum E_T^i \hat{n}_i$, where \hat{n}_i are the unit vectors pointing from the interaction point to the energy deposition in the calorimeter.
 - [8] F. Abe *et al.*, Phys. Rev. Lett. **74**, 2626 (1995).
 - [9] F. Abe *et al.*, Phys. Rev. Lett. **80**, 2767 (1998).
 - [10] T. Affolder *et al.*, "Measurement of the Top Quark Mass using the Collider Detector at Fermilab" (to be published).
 - [11] L. Demortier, R. Hall, R. Hughes, B. Klima, R. Roser, and M. Strovink, Fermilab Report No. Fermilab-TM-2084.
 - [12] F. Abe *et al.*, Phys. Rev. D **52**, 4784 (1995).
 - [13] F. Abe *et al.*, Phys. Rev. D **47**, 4857 (1993).
 - [14] J. Cassada, Ph.D. thesis, University of Rochester, 1999 (unpublished).
 - [15] F. A. Berends, W. T. Giele, H. Kuijf, and B. Tausk, Nucl. Phys. **B357**, 32 (1991).
 - [16] F. Abe *et al.*, Phys. Rev. D **59**, 092001 (1999).
 - [17] G. Marchesini and B. R. Webber, Nucl. Phys. **B310**, 461 (1998); G. Marchesini *et al.*, Comput. Phys. Commun. **67**, 465 (1992). We use HERWIG version 5.6.
 - [18] F. Ptohos (for the CDF collaboration), in *Proceedings of the International Europhysics Conference on High Energy Physics '99, Tampere, Finland, 1999* (Institute of Physics Publishing, Bristol, 2000).
 - [19] F. Abe *et al.*, Phys. Rev. Lett. **80**, 2773 (1998).
 - [20] T. Sjöstrand, Comput. Phys. Commun. **82**, 74 (1994). We use PYTHIA version 5.7.
 - [21] D. Cronin-Hennessy, A. Beretvas, and P. F. Derwent, Nucl. Instrum. Methods Phys. Res., Sect. A (to be published).